

Oxy-Combustion of Pulverized Coal: Modeling of Char-Combustion Kinetics

M. Geier¹, C. R. Shaddix¹, and B. S. Haynes²

¹Combustion Research Facility, Sandia National Labs, Livermore, CA 94550, USA

²School of Chemical and Biomolecular Engineering, University of Sydney, Sydney, NSW 2006, Australia

In this study, char combustion of pulverized coal under oxy-fuel combustion conditions was investigated on the basis of experimentally observed temperature-size characteristics and corresponding predictions of numerical simulations. Using a combustion-driven entrained flow reactor equipped with an optical particle-sizing pyrometer, combustion characteristics (particle temperatures and apparent size) of pulverized coal char particles was determined for combustion in both reduced oxygen and oxygen-enriched atmospheres with either a N₂ or CO₂ bath gas. The two coals investigated were a low-sulfur, high-volatile bituminous coal (Utah Skyline) and a low-sulfur subbituminous coal (North Antelope), both size-classified to 75–106 μm. A particular focus of this study lies in the analysis of the predictive modeling capabilities of simplified models that capture char combustion characteristics but exhibit the lowest possible complexity and thus facilitate incorporation in existing computational fluid dynamics (CFD) simulation codes. For this purpose, char consumption characteristics were calculated for char particles in the size range 10–200 μm using (1) single-film, apparent kinetic models with a chemically “frozen” boundary layer, and (2) a reacting porous particle model with detailed gas-phase kinetics and three separate heterogeneous reaction mechanisms of char-oxidation and gasification. A comparison of model results with experimental data suggests that single-film models with reaction orders between 0.5 and 1 with respect to the surface oxygen partial pressure may be capable of adequately predicting the temperature-size characteristics of char consumption, provided heterogeneous (steam and CO₂) gasification reactions are accounted for.

1. Introduction

Coal combustion using pure oxygen as the oxidizer appears to be an economically promising process for CO₂ separation for carbon capture and storage and has thus received considerable attention of the scientific community in recent years (e.g. [1-3] and references therein). Temperature control and material safety issues generally require a substantial degree of flue gas recycling, which yields elevated concentrations of carbon dioxide in the char combustion environment. Depending on whether the flue gas is dried before being recycled, higher moisture contents may be present as well. Flue gas recycling is particularly necessary for boiler retrofit applications, in which gas and particle temperatures similar to air-blown combustion are required to achieve the necessary heat transfer in different regions of the boiler. Due to the higher molar heat capacity of carbon dioxide

relative to nitrogen, flame temperatures for a given initial oxygen concentration are lower. Therefore, retrofitted boilers have to be operated at enhanced oxygen levels to maintain similar heat transfer rates [4,5]. Application of O₂-recycle combustion can cause differences in furnace operation parameters such as burner stability, char burnout, heat transfer and gas temperature profiles, as various pilot-scale tests have shown [4-12].

Computational fluid dynamics (CFD) simulations have become an indispensable tool during the process of designing and optimizing coal-fired boilers. CFD codes are frequently used to predict temperatures, heat transfer rates and species profiles in full-scale facilities, posing high demands on computational performance. For computations to provide results within practically acceptable time frames, reduced spatial resolution of the computational domain and simplified coal combustion models have to be used. The challenge in

this context is to develop models that are computationally inexpensive while still capturing all relevant information to produce realistic predictions. As most kinetics models and appropriate rate parameters have been derived for conventional, air-blown combustion systems, application of existing models for prediction of char burnout characteristics (particle temperatures and consumption rates) may yield erroneous results if char consumption in the oxy-combustion environment is influenced by additional reactions.

Recent computational results suggest that the the endothermic char gasification reaction $C(s) + CO_2 \rightarrow 2CO$ significantly reduces the temperature of pulverized coal chars burning at high temperatures in oxy-combustion environments [13]. The reaction affects the gas composition in the particle interior and, for 130 μm particles, leads to enhanced char consumption rates in environments with less than 24% oxygen. Similarly, simulations including the steam gasification reaction $C(s) + H_2O \rightarrow H_2 + CO$ show a reduction of char particle combustion temperatures, but a slight enhancement of the char consumption rate [14]. Simulation results further suggest that the partial conversion of CO to CO_2 in the particle boundary layer has an important influence on the char particle temperatures and burning rates under oxygen-enriched combustion conditions [15]. This is generally expected to be more important for larger particle sizes, as the characteristic diffusion time through the boundary layer increases for larger particles and thus provides more time for oxidation of CO to proceed.

The purpose of this study is to identify approaches for modification of existing single-film, n th-order apparent char kinetic models in order to accommodate differences in char consumption characteristics between conventional and oxy-fuel conditions. To this end, particles of two coals (a high-volatile bituminous and a subbituminous coal), sieved to 75-106 μm , are combusted in N_2 and CO_2 baths with different contents of O_2 , and experimentally observed temperature-size characteristics are compared with predictions of simple single-film models. Results of simulations with the porous particle combustion code SKIPPY are used to provide complementary information.

2. Experiment

2.1. Gas composition and temperature

Char consumption characteristics of pulverized coal was studied experimentally using Sandia's optical entrained flow reactor, described in more detail in [16]. The combustion-driven reactor relies on a diffusion-flamelet-based Hencken burner to produce a high-temperature gas flow at ambient pressure (1 atm). Solid fuel particles are introduced at the furnace centerline through a 0.75 mm stainless-steel tube by means of a small flow of N_2 or CO_2 , depending on the diluent used in the main reactant flow. For the experiments reported here, the coal feed rate was kept sufficiently low (~ 0.6 g/hr) to assure that injected particles burned in isolation from one another. The experimental setup further consists of a 46 cm tall 5 cm \times 5 cm quartz chimney that isolates the hot, post-combustion gas flow from the surrounding air and enables *in situ* optical measurements on the particles injected into the flow.

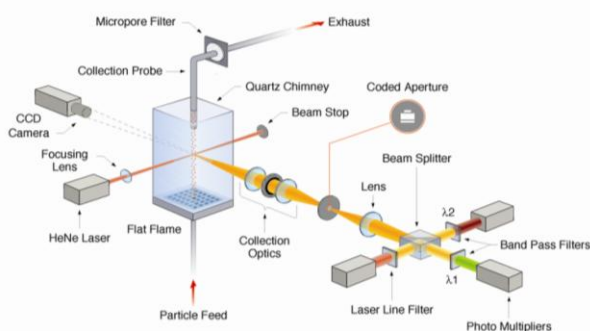


Figure 1 Schematic of Sandia's laminar entrained flow reactor for coal combustion studies. The particle-sizing pyrometry diagnostic is shown to the right of the flow reactor. Data collection is triggered by a particle passing through the focus of the HeNe laser beam along the centerline of the reactor.

For comparisons with predictions of different char combustion models, sieve-classified coal particles were entrained into mixtures with 12% (by mole), 24% or 36% O_2 , 16% moisture, and CO_2 or N_2 balance gas. Particle temperature-size data were collected at locations between 25 and 125 mm above the burner face, where gas temperatures were 1680 ± 40 K (see Figure 2). The gas temperature profile peaked at about 1700 ± 10 K at

50 mm above the burner surface and then decreased nearly linearly with increasing height (temperature profiles remained in a band of ± 10 K from the average gas temperature profile). The total burner product flow rate was 60 slpm (liters per minute at 0°C and 1 atm), which includes 0.03 slpm of diluent flow used for entraining the particles.

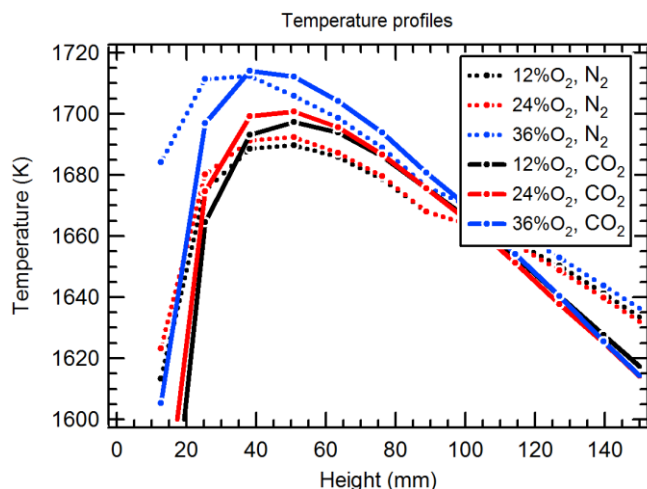


Figure 2 Radiation-corrected thermocouple measurements of gas temperature profiles in the entrained flow reactor. Measurements used a 25- μ m, type-R fine-wire thermocouple and were corrected for radiative losses following [17].

2.2. Fuels

The two coals investigated were a high-volatile bituminous coal (Utah Skyline) and a subbituminous coal from the Powder River Basin (North Antelope). Proximate and ultimate analyses of the pulverized coals are summarized in Table 1. For particle-sizing pyrometry, the coals, which are both considered low-sulfur coals, were sieved to 75-106 μ m to aid data acquisition. Additional analysis of three coal size fractions (53-75 μ m, 75-106 μ m and 106-125 μ m) confirmed size-independent elemental composition of ash contents.

3. Numerical Modeling

3.1. Detailed Char Consumption Model (SKIPPY)

SKIPPY (Surface Kinetics in Porous Particles) [18] is a FORTRAN program that calculates 1-D,

steady-state species concentration and temperature profiles of a single, porous, spherical particle placed in a quiescent, chemically reacting environment. Based on user-specified mechanisms for heterogeneous (gas-solid) and homogeneous reactions (e.g. GRIMECH 3.0 [19]), species concentrations and temperature inside the porous particle, at the external surface, and in the gas layer outside the particle are computed.

Table 1 Proximate and Ultimate Analysis of Coals

Proximate	Coal Type			
	Utah Skyline		North Antelope	
	wt%, as rec'd	wt% dry	wt%, as rec'd	wt% dry
moisture	3.18		23.69	
ash	8.83	9.12	4.94	6.47
volatiles	38.60	39.87	33.36	43.72
fixed C	49.39	51.01	38.01	49.81
Ultimate	wt% dry	wt% DAF	wt% dry	wt% DAF
C	70.60	77.44	53.72	56.51
H	5.41	5.93	6.22	6.54
O (by diff.)	13.21	14.49	34.11	35.88
N	1.42	1.56	0.78	0.82
S	0.53	0.58	0.23	0.24

The necessity of specifying reaction mechanisms makes SKIPPY a well-suited tool for studying the effects of reactions in the boundary layer (e.g. [15, 20]) or the importance of individual heterogeneous reactions (e.g. CO₂ gasification reaction on char consumption during oxy-fuel combustion of pulverized coal [13]). For the study presented here, we explored the effect of adding steam and CO₂ gasification reactions (R5 and R6 in Table 2) to the surface oxidation mechanism originally employed by Molina et al. [21]. In previous work (without gasification reactions), reactive specific char surface area was adjusted to bring observed and predicted temperatures of char particles burning in N₂ at different oxygen concentrations into agreement [15]. This approach resulted in a 24-fold reduction in surface area for char particles burning in 36% O₂ relative to those burning in 12% O₂. While there may be differences in surface areas of char formed *in situ* at differ-

ent bulk oxygen concentrations (due to differences in devolatilization characteristics), the variation in surface area that was required in those computations seems too large to be attributable to this phenomenon only. More likely, the simple heterogeneous reaction mechanism that was employed (char reaction with O_2 as the sole reactant) does not adequately model char surface reactions. Allowing for contributions by gasification reactions seems a reasonable approach, particularly for oxy-fuel combustion systems with flue gas recycling, where CO_2 (and possibly H_2O) concentrations can be considerably higher than in conventional combustion systems. The mechanism summarized in Table 2 is clearly an over-simplification (e.g. inhibition effects of CO and H_2 on the gasification reactions [22], rate-limiting effects of product desorption [23], and dependence of the CO/CO_2 production ratio on the concentration of O_2 at the surface [24] are not captured), but the goal here was to shed some light onto the relative importance of oxidation and gasification reactions in oxy-fuel versus conventional pulverized-coal combustion systems.

Table 2 Reaction rate constant parameters for the heterogeneous reactions used for SKIPPY simulations. The rate constants are specified in terms of Arrhenius expressions with pre-exponential factors A and activation energy E . The use of “_s” denotes species bond to surface sites, and “C(b)” denotes (inaccessible) bulk carbon atoms.

Reaction	A ($g/cm^2 s$)	E (kJ/mol)
Heterogeneous oxidation:		
(R1) $C_s + O_2 \Rightarrow CO + O_s$	3.3E+15	167.4
(R2) $O_s + 2C(b) \Rightarrow CO + C_s$	1.0E+08	0.
(R3) $C_s + O_2 \Rightarrow O_{2_s} + C(b)$	9.5E+13	142.3
(R4) $O_{2_s} + 2C(b) \Rightarrow C_s + CO_2$	1.0E+08	0.
CO ₂ gasification reaction:		
(R5) $C_s + CO_2 \Rightarrow CO + O_s + C(b)$	3.60E+15	251.0
Steam gasification reaction:		
(R6) $C_s + H_2O \Rightarrow H_2 + O_s + C(b)$	4.35E+14	222.8

In order to compare predictions and observations, char particle temperatures were computed for the size range 10 - 200 μm . The SKIPPY simulations used GRIMECH 3.0 [19] without nitrogen reactions and used the heterogeneous reactions listed in Table 2, with the rate parameters of R5 and R6 varied to assess the importance of these reactions. Internal specific surface area was held

constant for all particle sizes and O_2 concentrations; a value of 10 m^2/g was used to crudely reproduce temperatures for 100 μm particles burning in 12% O_2 . At this condition, particle temperatures are around 1900 K, which is relatively low to expect appreciable effect of the high activation energy gasification reactions [13-14]. Further simulation input parameters include bulk density = 560 kg/m^3 , tortuosity = 5, void fraction = 0.4, particle thermal conductivity = 1.33 $W/m \cdot K$, emissivity = 0.8, wall temperature (for radiative heat transfer) = 500 K, pressure = 101 kPa and gas temperature = 1690 K.

3.2. Simplified Char Consumption Model

Kinetic parameters for calculating the rate of char consumption can be obtained from measured data and an appropriate char consumption model. In the case of optical measurements on individually burning char particles carried by a hot gas flow, the char consumption process is governed by mass and heat transfer to and from the particle, as well as chemical reactions, both on the particle surface and in the gas phase. Mathematical models of considerable complexity can certainly be formulated to fully describe the overall process. However, using these models to estimate the rate parameters of heterogeneous reactions (a) requires accurate specification of imperfectly known model details (such as gas phase reaction rates, transport properties, pore structure, etc.), and (b) yields kinetics rate parameters that can produce poor predictions if utilized directly with simplified models of CFD codes. For those reasons, we compare measured temperature-size data with predictions from a relatively simple burnout model, as outlined below.

A simplified model, similar to those typically employed in CFD codes, was derived from the instantaneous energy balance on a homogeneous, chemically reacting, spherical particle. Assuming negligible effect of reactions in the boundary layer, average gas-mixture properties, and the overall char reaction $C + (1+\psi)/2 O_2 \rightarrow \psi CO_2 + (1-\psi) CO$, the instantaneous energy balance is given by (see [25] for more detail):

$$\frac{d_p \rho_p c v_p}{6} \frac{dT_p}{dz} = -\varepsilon \sigma (T_p^4 - T_w^4) - \frac{2\lambda}{d_p} \left[\frac{\kappa/2}{e^{\kappa/2} - 1} \right] (T_p - T_g) + q \Delta h$$

The left-hand term in this equation represents the thermal inertia of the particles, with particle diameter d_p (m), particle bulk density ρ_p (kg/m³), specific heat c (J/kg·K), particle speed v_p (m/s), surface temperature T_p (K), and spatial coordinate z (m). For the current set of measurements, the particle temperatures are nearly independent of the distance from the burner face, allowing this term to be neglected. The first term on the right represents radiative heat loss, with char emissivity ε and wall temperature T_w (K). The second term on the right represents convective heat loss of the particle, with mixture thermal conductivity λ (W/m·K), free-stream gas temperature T_g (K) and $\kappa = (-q \cdot d_p / \lambda) \sum_i v_i c_{g,i}$, which characterizes the heat transfer correction due to Stefan flow [25] (v_i are stoichiometric coefficients, with $v_{O_2} = (1+\psi)/2$, $v_{CO} = -(1-\psi)$, and $v_{CO_2} = -\psi$; $c_{g,i}$ are the corresponding specific heat capacities (J/kg·K)). The chemical heat release is represented by the far right-hand term, where q denotes the overall burning rate per unit external surface area (kg/m²·s), and $\Delta h = (1-\psi) \Delta h_{CO} + \psi \Delta h_{CO_2}$ is the overall heat of reaction (J/kg). The CO₂/CO production ratio at the char particle surface is modeled as $CO_2/CO \equiv \psi/(1-\psi) = 0.02 p(O_{2,s})^{0.21} \exp(3070/T_p)$ [24], where $p(O_{2,s})$ is the oxygen partial pressure at the particle surface (atm). $p(O_{2,s})$ follows from solution of the gas-phase diffusion equation [25] as $p(O_{2,s})/p = \gamma + [p(O_{2,\infty})/p - \gamma] \exp[-q/(\gamma k_d p)]$, where $\gamma = -(1+\psi)/(1-\psi)$, $p(O_{2,\infty})$ is the free-stream oxygen partial pressure (atm), $k_d = 2 \cdot W_C \cdot D_{O_2,mix} / (d_p \cdot R \cdot T_f \cdot v_{O_2})$ is the oxygen mass transfer coefficient (kg/m²·s·atm) with $W_C = 12$ g/mol, $D_{O_2,mix}$ is the mixture-averaged oxygen diffusion coefficient (m²/s), $R = 8.3144$ J/mol·K is the universal gas constant, and $T_f = (T_p + T_g)/2$ is the film temperature (K). Gas properties (λ , $D_{O_2,mix}$, and c_g) were calculated for $T = T_f$, and the free-stream gas composition as outlined in [26] (κ was approximated as $\kappa \approx -q \cdot d_p \cdot c_g \cdot W_C / (\gamma \cdot \lambda \cdot v_{O_2})$).

The surface-specific burning rate q , is typically expressed as

$$q = k_s(T_p) p_{O_2,s}^n$$

where $k_s(T_p) = W_C \cdot A \cdot \exp(-E/RT_p)$ in units of kg/m²·s·atm ^{n} , n is the reaction order, and the pre-exponential factor A is expressed in units of kmol/m²·s. This is the “ n th-order Arrhenius” expression of global char kinetics. For Zone-II combustion conditions, as are typically found for pulverized coal combustion, the diffusion of oxygen through the boundary layer has some influence on the burning rate of the particle, but the influence is not controlling the rate. However, the oxygen diffusion profile needs to be accounted for when calculating the surface concentration of oxygen.

For the study presented here, temperature-size characteristics were calculated with the described model. The required rate parameters A and E to specify q were determined for three reaction orders $n = 1, 0.5$ and 0.1 such that observed temperatures of 100 μ m particles burning in N₂ with 12% and 36% O₂ in the free stream were reproduced. Particle temperatures were then computed for sizes from 10 to 200 μ m for the experimental conditions studied (either CO₂ or N₂ diluent, 16% H₂O and three O₂ bulk concentrations (12%, 24%, 36%)). A gas temperature $T_g = 1690$ K, radiative boundary $T_w = 500$ K, and char particle emissivity $\varepsilon = 0.8$ were assumed. The obtained rate parameters are summarized in Table 3.

Table 3 Estimated rate parameters for North Antelope and Utah Skyline for the simplified steady-state burning model.

North Anthelope:		
Fixed $n =$	A (kmol/m ² ·s)	E (kJ/mol)
1	0.44	0.00
0.5	0.67	36.50
0.1	1.70	76.26
Utah Skyline:		
1	0.39	11.95
0.5	1.05	51.75
0.1	2.31	83.54

4. Results and Discussion

4.1. Single-film char consumption models

Figure 3 shows the results from the simplified model calculations for different reaction orders together with measured data for char particles

burning in N_2 diluent. Temperatures are significantly higher for the subbituminous North Antelope char (top), for which considerably smaller sizes were also measured (most likely due to a stronger tendency to fragment than the bituminous Utah Skyline char (bottom)). The overall spread of temperatures of Utah Skyline char particles is larger for a given reactor condition, which may reflect a higher variability in mineral contents of the coal particles.

For both North Antelope and Utah Skyline char, the calculated temperatures agree well near the “design” diameter $100\ \mu\text{m}$, but the diameter range for which predictions are reasonably good appears to be wider for reaction orders of $n = 0.5$ and $n = 1$. According to classical Thiele analysis, apparent reaction orders are constrained to lie between 0.5 and 1 for Zone II combustion [27,28], even though smaller reaction orders have been obtained in regression procedures for estimation of rate parameters (e.g. [25]) and ash-inhibition or similar processes that decrease reactivity with burnout can result in low effective reaction order [29]. The results shown in Figure 3 suggest that the predictions with $n = 0.1$ hold for sizes larger than $100\ \mu\text{m}$, and thus could be used in CFD models as long as the kinetics rates are not applied to particle sizes outside that range. Choosing a smaller particle size when estimating the rate parameters would have improved the predictions at smaller sizes, but at the cost of over-predicting temperatures for larger sizes. Given the observed nearly size-independent temperatures, it is recommended to keep reaction orders in the range between 0.5 and 1, to obtain more realistic profiles over the entire size range. However, the activation energies that are required when fitting the simulations to the data for high reaction orders can be very small (e.g. for $n = 1$, $E = 11.95\ \text{kJ/mol}$ and $0\ \text{kJ/mol}$ for North Antelope and Utah Skyline, respectively) and should be viewed as pure fitting parameters without practical meaning. But fitted parameters that strongly deviate from a physically realistic range indicate that the fitted model does not fully capture all relevant physical processes.

Figure 4 shows predicted and measured particle temperatures as a function of particle diameter for char particles burning in CO_2 -dominated gas mix-

tures. Compared with the data for N_2 diluent (Figure 3), the measured temperatures for both chars are lower in the CO_2 environment, consistent with previous findings [15]. Interestingly, for each free-stream oxygen concentration the char temperatures show a much wider spread about an average temperature-size profile than for the N_2 environment. This may be caused by differences in properties of *in situ* char produced in N_2 and CO_2 , but further investigation is necessary to clarify this point.

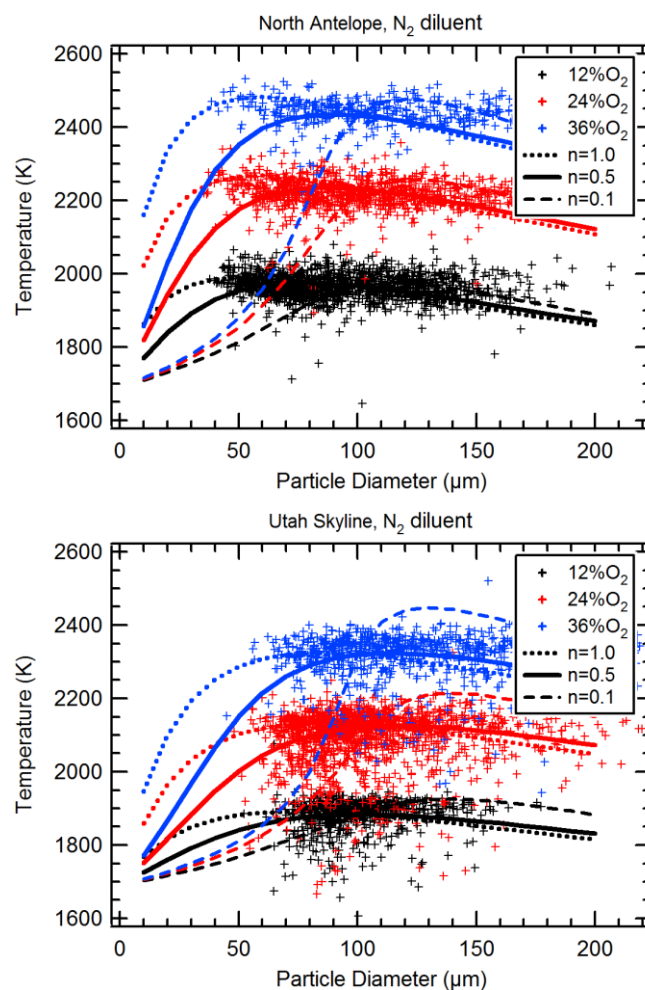


Figure 3 Predicted and measured (symbols) particle surface temperatures for three free-stream O_2 concentrations, 16% moisture and N_2 bath gas. Solid lines $n = 0.5$, dotted lines $n = 1$, dashed lines $n = 0.1$.

As shown in Figure 4, predicted temperatures for reaction orders of $n = 0.5$ and $n = 1$ are too high for North Antelope char particles but agree reasonably well for Utah Skyline char. Although

the predictions are slightly better for $n = 1$, both models yield similarly good predictions. In interpreting the results for Utah Skyline char, two issues must be kept in mind. First, the measured temperatures for both N_2 and CO_2 experiments are ~ 150 K lower than for North Antelope char, thus potential contributions by gasification reactions are less significant for Utah skyline char. Second, due to the higher variability in measured temperatures (presumably a consequence of higher variability of mineral contents), average temperatures of $100 \mu\text{m}$ particles seem biased towards lower temperatures (see Figure 3). The increased spread of temperatures of char burning in a CO_2 bath further obscures clear interpretation of discrepancies between model and experimental data.

The over-prediction of temperatures for North Antelope char shown in Figure 4 clearly points to inadequacy of the simplified model. From a CFD modeling perspective, several modifications of the model without the need to include time-consuming calculations of temperature and multi-species profiles in the boundary layer could be conceived. The simplest option may be to use the simplified model as it is, but with a different set of rate parameters for CO_2 environments. While this is straightforward, the model may remain valid only in a narrow range of moisture and CO_2 concentrations if gasification reactions considerably affect particle temperatures and/or char consumption rates. The next level of complexity might thus be to include char gasification reactions in CFD codes.

4.2. SKIPPY Simulations

Simulated particle temperatures for combustion in N_2 -dominated environments and three different heterogeneous reaction mechanisms are shown in Figure 5. The first mechanism consists of oxidation reactions R1-R4 only, which, as mentioned earlier, results in vast over-prediction of particle temperatures at elevated oxygen concentrations. The temperatures of smaller particles are controlled by convective heat loss, whereas radiative losses cause the temperature to fall at the large-size end of the studied size range. Highest temperatures are predicted in the intermediate size range

between 30 and $70 \mu\text{m}$, with peak temperatures shifting towards smaller sizes with increasing free-stream oxygen concentration.

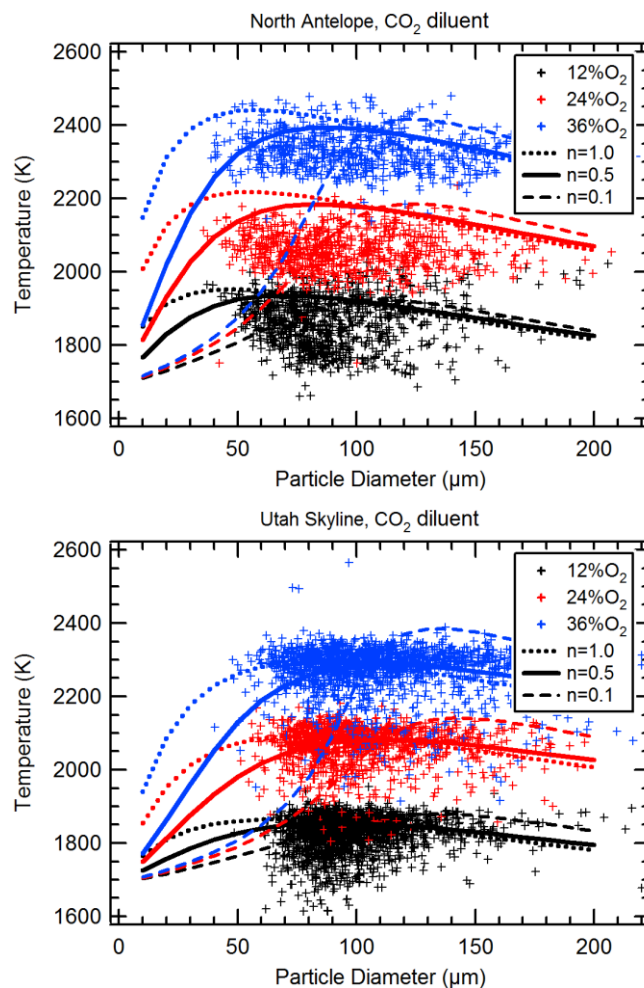


Figure 4 Predicted and measured (symbols) particle surface temperatures for three free-stream O_2 concentrations, 16% moisture and CO_2 bath gas. Solid lines $n = 0.5$, dotted lines $n = 1$, dashed lines $n = 0.1$.

The second mechanism includes R1-R4 and the steam gasification reaction, R6; however, in this case a different set of rate parameters was used for R6 than listed in Table 2: $A = 1.16E16 \text{ g/cm}^2 \cdot \text{s}$, and $E = 251.0 \text{ kJ/mol}$. This parameter set was found to produce the best match of predicted and observed temperatures of $100 \mu\text{m}$ particles and is still well within the range of activation energy and overall reaction rate that appears in the literature for steam gasification [14]. The relatively good fit for all oxygen bulk concentrations suggests that the steam gasification reaction plays an important

role in determining the char particle temperature and thereby the char oxidation rate.

The third model adds the CO_2 gasification reaction, R5, and thus uses the full mechanism specified in Table 2. Although the fit for 100 μm particles is slightly better than for the second model, the necessity of including this reaction is not obvious, based on the data shown in Figure 5 for N_2 -dominated environments.

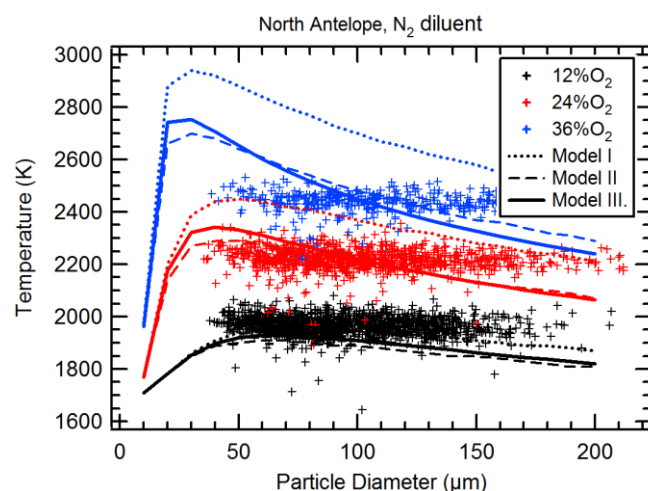


Figure 5 SKIPPY predictions of particle surface temperatures for three free-stream O_2 concentrations, 16% moisture and N_2 diluent compared with measured data for North Antelope char. Model I: oxidation only (R1-R4), Model II: oxidation with steam gasification (R6 with $E = 251 \text{ kJ/mol}$, $A = 1.16\text{E}16 \text{ g/cm}^2 \text{ s}$, Model III: R1-R6 as specified in Table 2.

Comparison of experimental data and model prediction for combustion in CO_2 diluent (Figure 6) clearly shows that both steam and CO_2 gasification reactions have to be included to produce an acceptable fit for sizes near 100 μm . Both reduced models (oxidation alone and oxidation together with steam gasification) over-predict temperatures for that size range. The suggested importance of CO_2 gasification implies that CO oxidation in the boundary layer, which produces additional CO_2 in the vicinity of the particle, may be more important than previously assumed. Similarly, the water-gas shift reaction ($\text{CO} + \text{H}_2\text{O} \rightarrow \text{CO}_2 + \text{H}_2$) might play a subtle role due to its impact on the gas composition near the particle surface. For combustion in conventional environments, the rate parameters for the steam gasification reaction had to be reduced

when adding the heterogeneous CO_2 reaction. This implies that CO_2 gasification plays an important role also when insignificant amounts of CO_2 are present in the bulk gas. Under those conditions, carbon dioxide formed at the char surface and in the boundary layer participates in gasification reactions (because of relative slow diffusion of CO_2 in N_2 , appreciable concentrations of CO_2 can be present at the particle surface despite low CO_2 production rates). For application to CFD codes, the suggested relevance of steam and CO_2 gasification reactions implies that lumped kinetics to model char consumption as a single-step oxidation process may only be valid for narrow ranges of combustion environments (in terms of steam and carbon dioxide concentrations). Therefore, it may be necessary to account for both steam and CO_2 concentrations to produce appropriate estimates of char temperatures and burning rates.

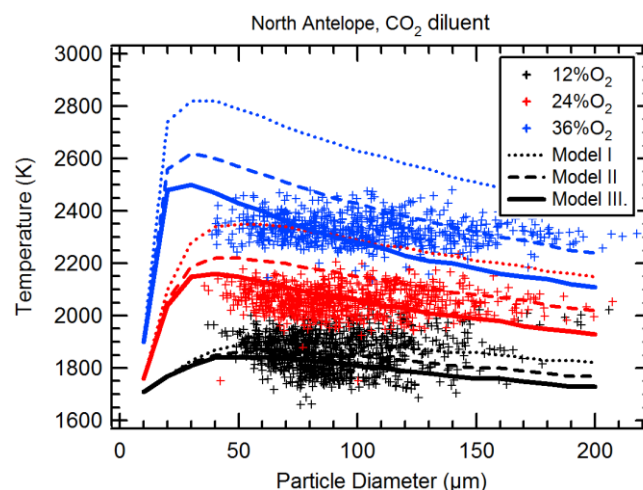


Figure 6 SKIPPY predictions (solid lines) of particle surface temperatures for three free-stream O_2 concentrations, 16% moisture and CO_2 diluent compared with measured data for North Antelope char. Model I: oxidation only (R1-R4), Model II: oxidation with steam gasification (R6 with $E = 251 \text{ kJ/mol}$, $A = 1.16\text{E}16 \text{ g/cm}^2 \text{ s}$, Model III: R1-R6 as specified in Table 2.

5. Summary

Combustion of char particles of bituminous (Utah Skyline) and subbituminous (North Antelope) coal in N_2 and CO_2 dominated gas environments with 12 to 36 mole-% O_2 and 16% H_2O were investigated both experimentally and through numerical simulations. Particle temperatures from

two-color pyrometer measurements were compared with predictions from (1) a simplified single-film apparent kinetics model, and (2) a more complex model that includes both homogeneous reactions of gas phase species and heterogeneous reactions in pores and external particle surface. Single-film model predictions suggest that optimized rate parameters for any reaction order between 0.5 and 1 produce reasonably good fits to the data and may thus be employed in CFD codes for wide size and temperature ranges. Particle temperatures for CO₂-dominated environments are generally over-predicted when using rate parameters derived with N₂ data, i.e. the simplified model investigated does not fully capture the characteristics of char consumption in oxy-fuel combustion conditions. As an alternative to the option of estimating separate sets of rate parameters for CFD applications in N₂-dominated and CO₂-dominated environments, heterogeneous steam and CO₂ gasification reactions could be included to improve the quality of the predictions.

Using the reacting particle simulation code SKIPPY (Surface Kinetics in Porous Particles), temperatures for particles around 100 μm were reasonably well predicted for both N₂ and CO₂ environments if both steam and CO₂ gasification reactions were included and a fixed reactive surface area of 10m²/g assumed. The results suggest that oxidation and both steam and CO₂ gasification reactions contribute to the char consumption process. An important conclusion therefore is that simplified (single-film) models must account for gasification reactions to maintain predictive capability in both combustion environments. To further substantiate these conclusions, experiments with externally prepared char (to remove effects of the combustion environment on devolatilization characteristics (and hence char properties)) will be conducted. In addition, a more sophisticated oxidation mechanism will be implemented to improve the quality of SKIPPY predictions.

Acknowledgement

This research was sponsored by the U.S. Department of Energy's Carbon Sequestration Program under award number DE-NT0005288. This work is part of a project led by Reaction Engineering International and is managed by Mr.

Timothy Fout of the National Energy Technology Laboratory. Sandia is a multiprogram laboratory operated by Sandia Corporation, a Lockheed Martin Company, for the United States Department of Energy's National Nuclear Security Administration under Contract DE-AC04-94AL85000.

Disclaimer

This report was prepared as an account of work sponsored by an agency of the United States Government. Neither the United States Government nor any agency thereof, nor any of their employees, makes any warranty, express or implied, or assumes any legal liability or responsibility for the accuracy, completeness, or usefulness of any information, apparatus, product, or process disclosed, or represents that its use would not infringe privately owned rights. Reference herein to any specific commercial product, process, or service by trade name, trademark, manufacturer, or otherwise does not necessarily constitute or imply its endorsement, recommendation, or favoring by the United States Government or any agency thereof. The views and opinions of authors expressed herein do not necessarily state or reflect those of the United States Government or any agency thereof.

References

- [1] B.J.P. Buhre, L.K. Elliott, C.D. Sheng, R.P. Gupta, T.F. Wall, *Prog. Energy Combust. Sci.* 31 (4) (2005) 283-307.
- [2] R. Tan, G. Corragio, S. Santos, *Oxy-Coal combustion with flue gas recycle for the power generation industry. A literature review*, Report No. IFRF Doc. No. G 23/y/1, International Flame Research Foundation, 2005.
- [3] M.B. Toftegaard, J. Brix, P.A. Jensen, P. Glarborg, A.D. Jensen, *Prog. Energy Combust. Sci.* 36 (2010) 581-625.
- [4] R. Payne, S.L. Chen, A.M. Wolsky, W.F. Richter, *Combust. Flame* 67 (1989) 1-16.
- [5] H. Liu, R. Zailani, B.M. Gibbs, *Fuel* 84 (16) (2005) 2109-2115.
- [6] T. Kiga, S. Takano, N. Kimura, K. Omata, M. Okawa, T. Mori, M. Kato, *Energy Conv. Managmt.* 38 (0) (1997) S134.
- [7] T. Nozaki, S. Takano, T. Kiga, K. Omata, N. Kimura, *Energy* 22 (2-3) (1997) 199-205.
- [8] H. Farzan, S.J. Vecci, F. Chatel-Pelage, P. Pranda, A.C. Bose, *Pilot-scale evaluation of coal combustion in an oxygen-enriched recycled flue gas*. The 30th international technical conference on coal utilization & fuel systems. Clearwater, FL, USA, 2005.
- [9] H. Liu, R. Zailani, B.M. Gibbs, *Fuel* 84 (7-8) (2005) 833-840.
- [10] S.P. Khare, T.F. Wall, A.Z. Farida, Y. Liu, B. Moghtaderi, R.P. Gupta, *Fuel* 87 (2008) 1042-1049.
- [11] X. Huang, X. Jiang, X. Han, H. Wang, *Energy & Fuels* 22 (2008) 3756-3762.
- [12] P. Heil, D. Toporov, H. Stadler, S. Tschunko, M. Förster, R. Kneer, *Fuel* 88 (2009) 1269-1274.
- [13] E. S. Hecht, C. R. Shaddix, A. Molina, B. S. Haynes *Proc. Combust. Inst.*, in press.

- [14] C.R. Shaddix, E.S. Hecht, M. Geier, A. Molina, B.S. Haynes, *Effect of gasification reactions on oxy-fuel combustion of pulverized coal char*, Proceedings of the 35th International Technical Conference on Clean Coal & Fuel Systems, Clearwater FL, June 6–10, 2010.
- [15] C.R. Shaddix, A. Molina, *Effect of O₂ and High CO₂ Concentrations on PC Char Burning Rates during Oxy-Fuel Combustion*, Proceedings of the 33rd International Technical Conference on Coal Utilization and Fuel Systems, Clearwater, FL, June 1-5, 2008.
- [16] D.A. Tichenor, S. Niksa, K.R. Hencken, R.E. Mitchell, *Proc. Combust. Inst.* 20:1213-1221 (1984).
- [17] C.R. Shaddix, “Correcting thermocouple measurements for radiation loss: A critical review,” 33rd National Heat Transfer Conference, Albuquerque, NM, USA, 1999, p. 1150.
- [18] P.J. Ashman, B.S. Haynes, *Improved techniques for the prediction of NO_x formation from char nitrogen*, Project No. C4065, Australian Coal Association. CSIRO Energy Technology, 1999.
- [19] G.P. Smith, S.D. Golden, M. Frenklach, N.W. Moriaty, B. Eitener, M. Goldenberg, C.T. Bowman, R.K. Hanson, S. Song, W.C. Gardiner, V.V. Lissianski, Z. Qin, (2001) GRI-MECH 3.0. http://www.me.berkeley.edu/gri_mech (accessed December 2001).
- [20] M. Geier, E.S. Hecht, C.R. Shaddix, *26th Annual International Pittsburgh Coal Conference, Pittsburgh PA Sept. 20-23, 2009*
- [21] A. Molina, A.F. Sarofim, W. Ren, J. Lu, G. Yue, J.M. Beer, B.S. Haynes, *Combust. Sci. Technol.* 174 (2002) 43-71.
- [22] N.M. Laurendeau, *Prog. Energy Combust. Sci.* 4 (1978) 221-270.
- [23] R.H. Essenhigh, *Energy & Fuels* 5 (1991) 41-46.
- [24] L. Tognotti, J.P. Longwell, A.F. Sarofim, *Proc. Combust. Inst.* 23 (1990) 1207-1213.
- [25] J.J. Murphy, C.R. Shaddix, *Combust. Flame* 144:710-729 (2006).
- [26] P.H. Paul, J. Warnatz, *Proc. Combust. Inst.* 27 (1998), 495–504.
- [27] E.W. Thiele, *Ind. Eng. Chem.* 31 (1939) 916–920.
- [28] M.F.R. Mulcahy, I.W. Smith, *Rev. Pure. Appl. Chem.* 19 (1969) 81–108.
- [29] J.J. Murphy, C.R. Shaddix, *Combust. Flame* 157: (2010) 535-539